JOURNAL OF MATERIALS SCIENCE **37** (2002) 977–982

# Synthesis of silica-coated rhodium nanoparticles in reversed micellar solution

T. TAGO, Y. SHIBATA, T. HATSUTA, K. MIYAJIMA, M. KISHIDA,
S. TASHIRO, K. WAKABAYASHI
*Department of Materials Process Engineering, Graduate School of Engineering,
Kyushu University, 6-10-1, Hakozaki, Higashi-Ku, Fukuoka 812-8581, Japan
E-mail: ttago@apex.chem-eng.kyushu-u.ac.jp*

Silica ($SiO_2$)-coated rhodium (Rh) nanoparticles were prepared using a water-in-oil microemulsion of polyoxyethylene (15) cetyl ether, cyclohexane and water. $SiO_2$-coated Rh nanoparticles were obtained by hydrolyzing metal alkoxide (tetraethylorthosilicate, TEOS) in the solution containing Rh complex nanoparticles followed by thermal and reduction treatments. In the $SiO_2$-coated Rh nanoparticle, a Rh particle with an average diameter of 4.1 nm was located nearly at the center of each spherical $SiO_2$ particle. The $SiO_2$ layer was approximately 15 nm thick. Since the Rh particle was wholly surrounded by $SiO_2$, the Rh particle of the $SiO_2$-coated Rh nanoparticle exhibited an extremely high thermal stability. Furthermore, the porous structure of the $SiO_2$ layer could be controlled by the hydrolysis conditions of TEOS.

## 1. Introduction

Recently, nanoparticles with a heterogeneous structure have attracted the attention of many researchers as a result of their superior physical and/or chemical properties in comparison with those of homogeneous nanoparticles. For example, the heterogeneous structure has been effective in the enhancement of chemical and colloidal stability [1, 2], luminescence of semiconductor nanoparticles [3, 4] and dispersion of ferrofluid [5]. Coating, one method of preparing the heterogeneous nanoparticle that has received a considerable attention, has been used with silica ($SiO_2$) in the field of sol-gel chemistry. Several groups have reported on the preparation of a $SiO_2$-coated metal [6–10], metal oxide [5, 11, 12] and metal compound [1, 13–15]. Liz-Marzán *et al.* [8–10] have employed the silane-coupling agent (3-aminopropyl trimethoxysilane) to form silane triols on the surface of gold and silver colloids, where the growth of a $SiO_2$ layer was promoted by adding a silica source. Kishida and Tago [16, 17] and Li *et al.* [7] have reported $SiO_2$-coated Rh and $SiO_2$-coated silver nanoparticles synthesized within reversed micellar solution via metal alkoxide hydrolysis, respectively. We describe here a method for preparing $SiO_2$-coated Rh nanoparticle using microemulsion [16, 17], and examine the thermal stability of Rh nanoparticles within $SiO_2$ particles. In addition, we report on our investigation of the effect of the hydrolysis condition of TEOS on the porous structure of the $SiO_2$ layer.

## 2. Experimental

The $SiO_2$-coated Rh nanoparticles were prepared using a water-in-oil (w/o) microemulsion. The nonionic surfactant, polyoxyethylene (15) cetyl ether (C-15), and ionic surfactants, sodium bis(2-ethylhexyl) sulfosuccinate (AOT) and cetyltrimethylammonium chloride (CTAC), were used in this study. Cyclohexane was used as an organic solvent except in the case of CTAC, because a CTAC/cyclohexane microemulsion could not be formed. 1-hexanol was used as an organic solvent in the case of CTAC. The concentration of surfactants in organic solvents was 0.5 mol/l. The microemulsion was prepared by injecting an aqueous rhodium trichloride ($RhCl_3 \cdot 3H_2O$, purity min. 99.9%) solution (0.38 mol/l, 2.6 ml) into the organic surfactant solution (100 ml) at 50°C. Nanoparticles of Rh-hydrazine ($N_2H_4$) complex were synthesized in the microemulsion by adding $N_2H_4$ hydrate (molar ratio of $N_2H_4$ to Rh = 3.0) directly into the w/o microemulsion. Tetraethylorthosilicate (TEOS, 0.86 mol/l) as a $SiO_2$ source and diluted ammonium ($NH_4OH$) solution (0.45–2.70 mol/l) were charged into the microemulsion, and the hydrolysis of TEOS was performed at 50°C. The molar ratio of water to surfactant in the solution during TEOS hydrolysis was 23. In order to terminate TEOS hydrolysis, the micellar structure of the solution containing $SiO_2$-coated Rh-hydrazine complex nanoparticles was destroyed by adding propanol to the solution. Then, the solution was centrifuged to separate the $SiO_2$ precipitate including Rh-hydrazine complex nanoparticles from the solution containing TEOS. The $SiO_2$ precipitate thus obtained was thoroughly washed with propanol, dried at 80°C overnight and calcined under air flow at 500°C for 2 hours in order to remove the surfactant. Finally, the samples thus obtained were reduced with $H_2$ at 450°C for 2 hours.

The precipitate containing Rh-$N_2H_4$ nanoparticles and the $SiO_2$-coated Rh nanoparticle were observed by transmission electron microscopy (TEM, Nihon Denshi

JEM-2000FX). For TEM study, the $SiO_2$-coated Rh nanoparticle (after air calcination and $H_2$ reduction) was ultrasonically dispersed in ethanol by adding drops of 2-dimethylaminoethanol as a dispersant, and the ethanol solution was dropped on a carbon film supported on a Cu grid. The BET surface area and pore size distribution of the nanoparticles were evaluated by measuring the nitrogen and argon sorption (Shimadzu ASAP-2010). The Rh particle size was determined by the X-ray line broadening technique (Rigaku RINT-2500) and by the pulse method using CO chemisorption on the surface of Rh particles.

## 3. Results and discussion

### 3.1. Preparation of the $SiO_2$-coated Rh nanoparticle

We investigated the morphology of the Rh-$SiO_2$ samples prepared using various surfactants. The samples were subjected to air calcination at 500°C and $H_2$ reduction at 450°C in order to remove the surfactant within the $SiO_2$ layer and to reduce the rhodium ion (rhodium oxide) to rhodium metal. Fig. 1a and b show the TEM photograph of the sample prepared using C-15/cyclohexane microemulsion. The $NH_4OH$ concentration during TEOS hydrolysis was 2.7 mol/l, and

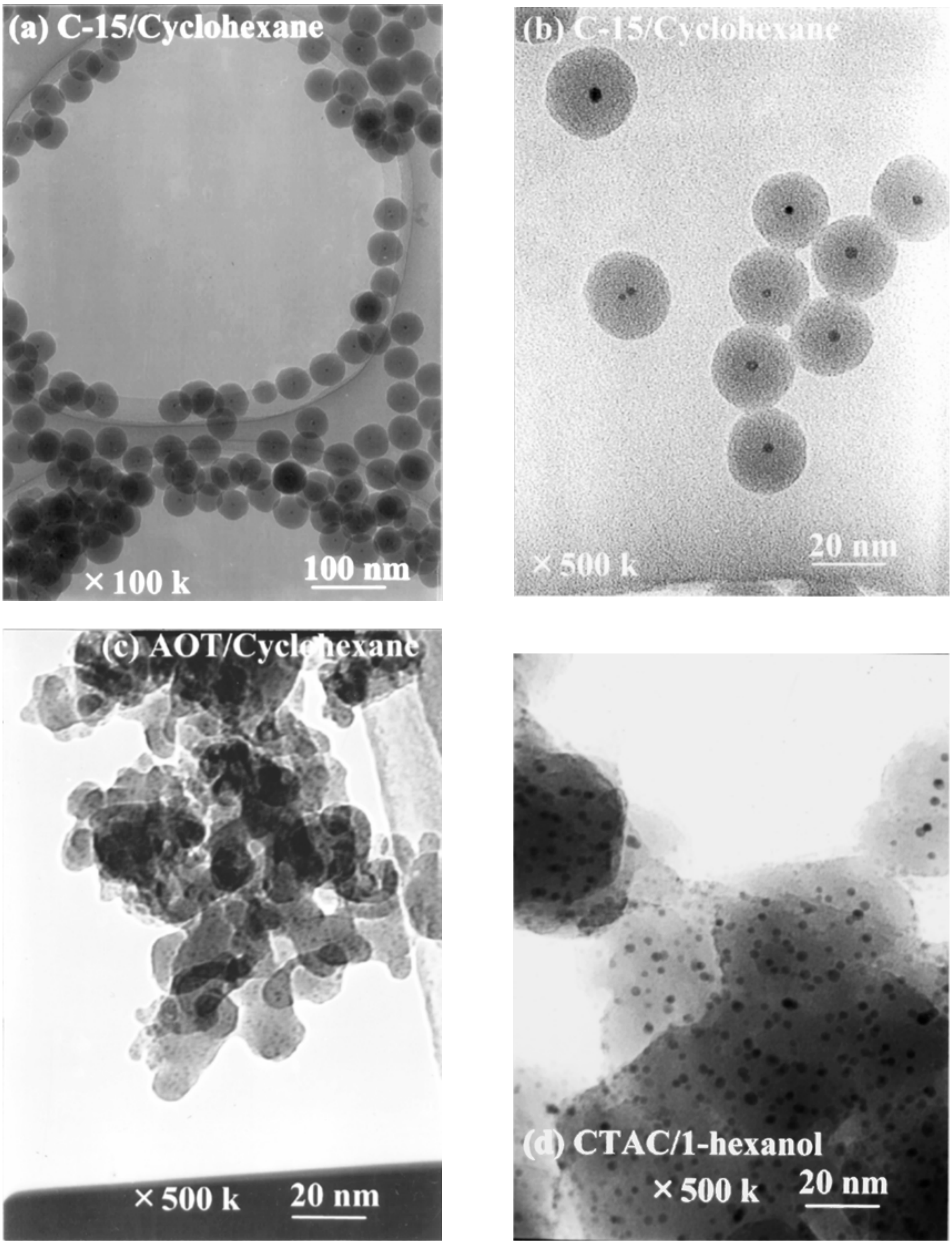

*Figure 1* TEM photographs of $SiO_2$-coated Rh nanoparticles prepared using (a, b) C-15, and Rh-$SiO_2$ samples prepared using (c) AOT and (d) CTAC after air calcination and $H_2$ reduction.

the hydrolysis time was 60 minutes. It was found that a Rh particle was located nearly at the center of each spherical $SiO_2$ particle, and that the respective particle sizes of Rh and $SiO_2$ were very uniform. The size of the centered Rh particle and the overall size of the $SiO_2$-coated Rh nanoparticle were 4.0 nm and 35 nm, respectively. Here, the thickness of the $SiO_2$ layer was approximately 15 nm.

The TEM photographs of the Rh-$SiO_2$ samples prepared using AOT and CTAC as surfactants are shown in Fig. 1c and d, respectively. Although the Rh particle sizes were nearly equal to that in the case of C-15, $SiO_2$ particles were irregular in shape and the Rh particles were randomly dispersed in $SiO_2$. As a result, the $SiO_2$-coated Rh nanoparticles were prepared using C-15/cyclohexane microemulsion.

As mentioned above, the $SiO_2$ precipitate containing Rh-$N_2H_4$ was subjected to air calcination and $H_2$ reduction (samples shown in Fig. 1), in contrast to the preparation method reported by Liz-Marzán [8–10], in which $SiO_2$-coated Au and Ag nanoparticles were prepared without air calcination. In order to compare our method with the previous method reported by Liz-Marzán, the $SiO_2$ precipitate containing Rh-$N_2H_4$ nanoparticles (before air calcination) obtained using C-15 was observed by TEM. For TEM study, the microemulsion solution containing the $SiO_2$ precipitate was diluted with ethanol under ultrasonic irradiation, and the ethanol solution was dropped on a carbon film supported on a Cu grid. Fig. 2 shows the TEM photographs of the precipitate. As can be seen from the figure, monodispersed $SiO_2$ particles (with an average diameter of 35 nm) including Rh-$N_2H_4$ nanoparticles (with an average diameter of 2.0 nm) were obtained. Accordingly, the air calcination and $H_2$ reduction were not essential in our preparation method for $SiO_2$-coated nanoparticles, as in the case of Liz-Marzán's method. Furthermore, as can be seen from the figure, each $SiO_2$ particle included a fixed number (an average number of 4) of Rh-$N_2H_4$ nanoparticles, and the nanoparticles were located near the center of each $SiO_2$ particle. This result indicates that the aggregation of Rh-$N_2H_4$ nanoparticles occurred via the $SiO_2$ nuclei when $SiO_2$ started to form from TEOS, and that the aggregation was completed at an early stage of the TEOS hydrolysis.

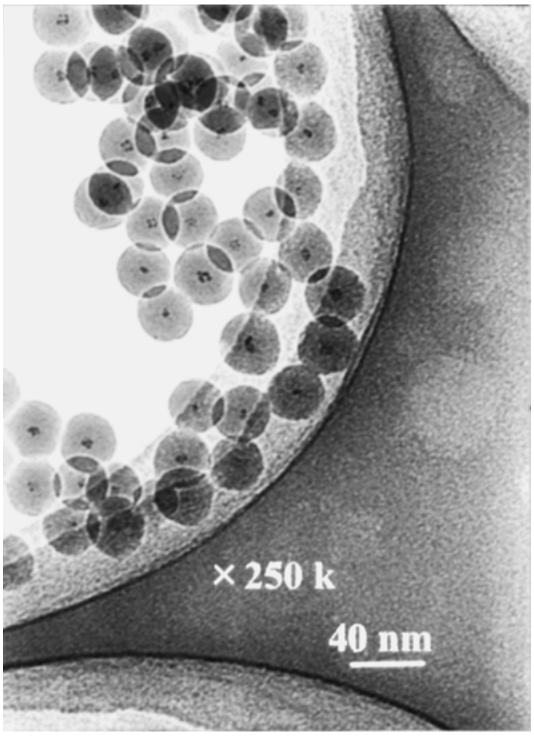

*Figure 2* TEM photographs of $SiO_2$ precipitate containing Rh-$N_2H_4$ nanoparticles prepared using C-15.

Fig. 3 shows the TEM photographs of the $SiO_2$-coated Rh nanoparticles prepared with hydrolysis times of 1, 5 and 30 minutes. The calcination and $H_2$ reduction temperatures were 500°C and 450°C, respectively. Notably, the Rh nanoparticle was coated with $SiO_2$ and located nearly at the center of the spherical $SiO_2$ at the initial hydrolysis time of 1 minute. Although the thickness of the $SiO_2$ layer increased with increasing hydrolysis time, the particle sizes of Rh were almost identical regardless of the hydrolysis time. These results confirmed that the aggregation of Rh-$N_2H_4$ nanoparticles via $SiO_2$ nuclei was completed at an early stage of the TEOS hydrolysis. Moreover, the thickness of the $SiO_2$ layer could be varied in the range of 4–25 nm by changing the hydrolysis time.

As can be seen from Fig. 1b, Figs 2 and 3, the Rh particle size of the $SiO_2$-coated Rh nanoparticle was larger than that of a Rh-$N_2H_4$ nanoparticle. The large size of Rh nanoparticles, in comparison with the size of Rh-$N_2H_4$ nanoparticles, resulted from the aggregation of Rh-$N_2H_4$ nanoparticles within each $SiO_2$ particle during the calcination and reduction process. Moreover, the size uniformity of Rh nanoparticles of $SiO_2$-coated Rh nanoparticles was correlated with almost the same number of Rh-$N_2H_4$ nanoparticles including a $SiO_2$ particle.

Fig. 4a shows the x-ray diffraction pattern of the $SiO_2$-coated Rh nanoparticle. The peaks corresponding to those of Rh metal at $2\theta = 41.0^\circ$ and $47.8^\circ$ were observed, and the average particle size calculated by the broadening technique was 4.1 nm, which was in good agreement with the particle size obtained from the TEM photograph.

### 3.2. Thermal stability of the $SiO_2$-coated Rh particle

Nanometer-sized noble metal particles such as Pt, Pd and Rh are commercially used as catalysts, e.g., automotive catalyst. However, these metal particles are easily aggregated at high temperature, leading to the decrease in catalytic activity. In order to investigate the thermal stability of the Rh particle of the $SiO_2$-coated Rh nanoparticle, the particle was subjected to calcination under airflow at 800°C and 1000°C for 2 h, then again reduced with $H_2$ at 450°C for 2 h. The dashed and solid lines in Fig. 4b represent the pattern of the particles after air calcination (800°C and 1000°C) and $H_2$ reduction (450°C), respectively. The peaks corresponding to those of Rh metal completely disappeared after air calcination and were subsequently observed after $H_2$ reduction, indicating that gases could reach the centered Rh surface through the $SiO_2$ layer, and

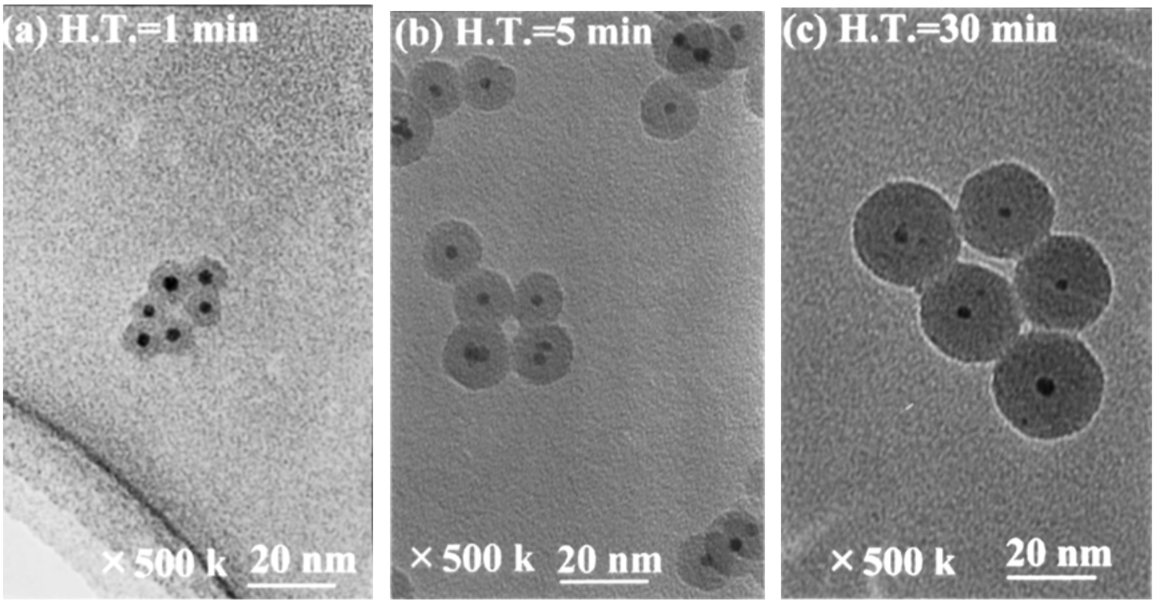

*Figure 3* TEM photographs of $SiO_2$-coated Rh nanoparticles prepared with hydrolysis times of (a) 1, (b) 5 and (c) 30 minutes.

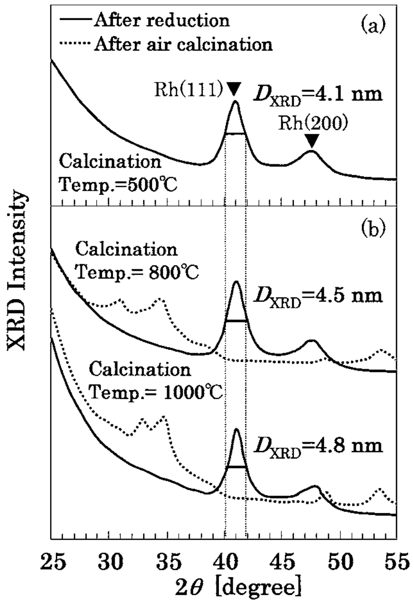

*Figure 4* X-ray diffraction patterns of the $SiO_2$-coated Rh nanoparticles after air calcination and $H_2$ reduction. The calcination temperatures were (a) 500°C, (b) 800°C and (c) 1000°C.

that the $SiO_2$ layer possessed a porous structure. The half-peak widths of the (111) plane, which were used to calculate an average particle size by the broadening technique, were almost identical regardless of the calcination temperature. The Rh particle sizes were 4.5 and 4.8 nm at calcination temperatures of 800°C and 1000°C, respectively.

Fig. 5 shows the TEM photographs of the $SiO_2$-coated Rh nanoparticles shown in Fig. 4b. The spherical $SiO_2$ structure remained almost unchanged, and the Rh particle size observed from the TEM photograph was in good agreement with that determined by the X-ray broadening technique. Accordingly, high thermal stability of the Rh particle resulted from the structure of the $SiO_2$-coated Rh nanoparticles. Since the Rh particle was wholly surrounded by $SiO_2$, the Rh particle had a strong resistance to sintering at high temperature.

However, as can be seen from Fig. 5, the $SiO_2$ particles were partly connected with each other, which was not observed from the samples after air calcination below 500°C shown in Figs 1 and 3, and monodispersed $SiO_2$ containing Rh particles could not be obtained after air calcination at 800°C and 1000°C.

### 3.3. Change in porous structure of the $SiO_2$ layer

As discussed above, it was found that the $SiO_2$ layer of the $SiO_2$-coated Rh particles had a porous structure, and that the Rh particle within the spherical $SiO_2$ particle was in contact with the gas phase. In this study, the ratio of the Rh metals in contact with the gas phase to the Rh metals composing the total surface of Rh particles was defined as the $R$-value, and the ratio was calculated using the following equation:

$$R = \frac{\left(\begin{array}{c}\text{Rh metal in contact with the gas phase:}\\ \text{determined by CO chemisorption}\end{array}\right)}{\left(\begin{array}{c}\text{Rh metal composing the total surface of Rh particles:}\\ \text{determined by X-ray diffraction analysis}\end{array}\right)}. \tag{1}$$

The controllability of the $R$-value and $SiO_2$ porous structure is very important for the application of $SiO_2$-coated nanoparticles. Increasing the $R$-value and pore volume will increase the catalytic activity of $SiO_2$-coated nanoparticles [18]. A small pore volume in $SiO_2$ cells hinders the centered particles from oxidizing. For example, the centered magnetite ($Fe_3O_4$) particle of the $SiO_2$-coated $Fe_3O_4$ nanoparticles had a high resistance to oxidation compared with $Fe_3O_4$ particles without $SiO_2$ cells [19, 20].

It appears that the $R$-value can be changed by changing the porous structure of the $SiO_2$ layer, which is affected by the hydrolysis condition of TEOS [21, 22], e.g., the $NH_4OH$ concentration. With that in mind, we investigated the effect of $NH_4OH$ concentration during TEOS hydrolysis on the $R$-value, BET surface area and pore size distribution of the particles.

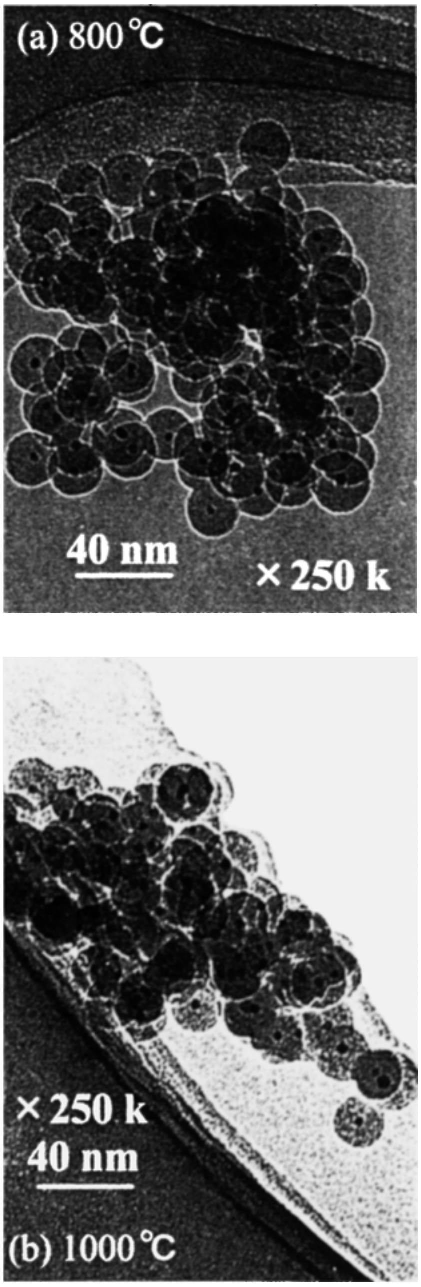

*Figure 5* TEM photographs of $SiO_2$-coated Rh nanoparticles after air calcination and $H_2$ reduction. The calcination temperatures were (a) 800°C and (b) 1000°C.

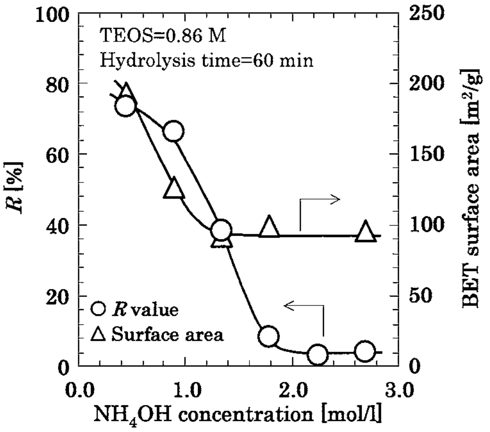

*Figure 6* Effect of $NH_4OH$ concentration on $R$-value and BET surface area of $SiO_2$-coated Rh nanoparticles.

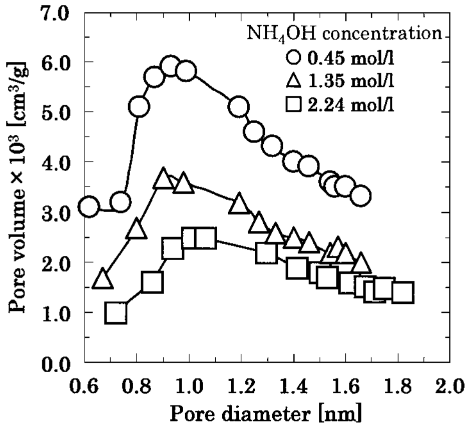

*Figure 7* Pore size distributions of $SiO_2$-coated Rh nanoparticles prepared with different $NH_4OH$ concentrations during TEOS hydrolysis.

Fig. 6 shows the $R$-value and the BET surface area of the $SiO_2$-coated Rh nanoparticles as a function of $NH_4OH$ concentration. When no $NH_4OH$ solution was added, the hydrolysis rate of TEOS was very slow and the $SiO_2$ layer around the Rh particle was not formed. As shown in this figure, the $NH_4OH$ concentration during TEOS hydrolysis affected the $R$-value and the BET surface area, both of which were increased with decreasing $NH_4OH$ concentration. The $R$-value reached approximately 73% at the $NH_4OH$ concentration of 0.45 mol/l. Fig. 7 shows the pore size distributions of the $SiO_2$-coated Rh nanoparticles. The average pore diameters were approximately 1.0 nm and were identical in size regardless of the $NH_4OH$ concentration. However, the pore volume was increased with decreasing $NH_4OH$ concentration, indicating that the increase in BET surface area resulted from the increase in pore volume. Accordingly, these results suggest that the development of the porous structure of $SiO_2$ in response to the change in the $NH_4OH$ concentration led to the increase in $R$-value. The $R$-value could be controlled in the range of 3.0%–73%.

## 4. Conclusion

We prepared $SiO_2$-coated Rh nanoparticles using a water-in-oil microemulsion of polyoxyethylene (15) cetylether, cyclohexane and water. A Rh particle was located nearly at the center of each spherical $SiO_2$ particle, and the particle sizes of Rh (4.1 nm) and $SiO_2$ (35 nm) were very uniform. Via TEM observation of the precipitate containing Rh-$N_2H_4$ nanoparticles, it was found that a fixed number of Rh-$N_2H_4$ nanoparticles were located near the center of each spherical $SiO_2$ particle, indicating that the aggregation of Rh-$N_2H_4$ nanoparticles occurred via $SiO_2$ nuclei. Investigation of the morphology of $SiO_2$-coated Rh nanoparticles with different hydrolysis times indicated that the aggregation was completed at an early stage of the TEOS hydrolysis.

We also investigated the thermal stability of the $SiO_2$-coated Rh nanoparticles. The Rh particle size of $SiO_2$-coated Rh nanoparticles was almost unchanged, even though the particles were calcined at 800°C and 1000°C. Furthermore, the porous structure of the $SiO_2$

layer could be changed by adjusting the $NH_4OH$ concentration during TEOS hydrolysis. The pore volume and BET surface area were increased with decreasing $NH_4OH$ concentration, which led to an increase in $R$-value.

## Acknowledgements

The authors would like to thank the Research Laboratory of High Voltage Electron Microscopy, Kyushu University, for the transmission electron micrograph. This work was supported in part by a Grant-in-Aid for Exploratory Research (No. 10875152) from the Ministry of Education, Science, and Culture.

## References

1. M. A. CORREA-DUARTE, M. GIERSIG and L. M. LIZ-MARZÁN, *Chem. Phys. Lett.* **286** (1998) 497.
2. I. PASTORIZA-SANTOS and L. M. LIZ-MARZÁN, *Langmuir* **15** (1999) 948.
3. M. A. HINES and P. GUYOT-SIONNEST, *J. Phys. Chem.* **100** (1996) 468.
4. X. G. PENG, M. C. SCHLAMP, A. V. KADAVANICH and A. P. ALIVISATOS, *J. Am. Chem. Soc.* **119** (1997) 7019.
5. A. P. PHILIPSE, A. M. NECHIFOR and C. PATHMAMANOHARAN, *Langmuir* **10** (1994) 4451.
6. M. GIERSIG, T. UNG, L. M. LIZ-MARZÁN and P. MULVANEY, *Adv. Mater.* **9** (1997) 570.
7. T. LI, J. MOON, A. A. MORRONE, J. J. MECHOLSKY, D. R. TALHAM and J. H. ADAIR, *Langmuir* **15** (1999) 4328.
8. L. M. LIZ-MARZÁN and A. P. PHILIPSE, *J. Colloid Interface Sci.* **176** (1995) 459.
9. L. M. LIZ-MARZÁN, M. GIERSIG and P. MULVANEY, *Langmuir* **12** (1996) 4329.
10. *Idem.*, *Chem. Commun.* (1996) 731.
11. M. A. CORREA-DUARTE, M. GIERSIG, N. A. KOTOV and L. M. LIZ-MARZÁN, *Langmuir* **14** (1998) 6430.
12. M. OHMORI and E. MATIJEVIC, *J. Colloid Interface Sci.* **150** (1992) 594.
13. P. MULVANEY, M. GIERSIG and A. HENGLEIN, *J. Phys. Chem.* **97** (1993) 7061.
14. N. TOSHIMA, *Pure Appl. Chem.* **72** (2000) 317.
15. *Idem.*, *Macromol. Symp.* **156** (2000) 45.
16. M. KISHIDA, N. NAKATA, S. TASHIRO and K. WAKABAYASHI, in Proceedings of the 3rd Tokyo Conference on Advanced Catalytic Science and Technology, Tokyo, July, 1998, Organized by Catalysis Society of Japan (Tokyo, Japan, 1998) p. 426.
17. M. KISHIDA, T. TAGO, T. HATSUTA and K. WAKABAYASHI, *Chemistry Letters* (2000) 1108.
18. M. IKEDA, T. TAGO, M. KISHIDA and K. WAKABAYASHI, *Chemical Communications*, accepted.
19. T. TAGO, R. NAGASE, T. HATSUTA, M. KISHIDA and K. WAKABAYASHI, in *Proceedings of the Eighth International Conference on Ferrite*, Kyoto, August 2000, Organized by Japan Society of Powder and Powder Metallurgy (Tokyo, Japan, 1998) p. 763–765.
20. T. TAGO, T. HATSUTA, K. MIYAJIMA, M. KISHIDA, S. TASHIRO and K. WAKABAYASHI, *J. Amer. Ceram. Soc.*, submitted.
21. M. KISHIDA, K. ONOUE, S. TASHIRO, H. NAGATA and K. WAKABAYASHI, *Studies Surface Sci. Catal.* **114** (1998) 411.
22. M. KISHIDA, T. HANAOKA, H. NAGATA and K. WAKABAYASHI, *Catalysis Today* **45** (1998) 203.

*Received 2 February*
*and accepted 22 October 2001*